



Synthesis of Co³⁺ Doped TiO₂ by Co-precipitation Route and Its Gas Sensing Properties

Roussin Lontio Fomekong and Bilge Saruhan*

Department of High-Temperature and Functional Coatings, German Aerospace Center (DLR), Institute of Materials Research, Cologne, Germany

Undoped and Co-doped TiO₂ nanoparticles were synthesized by a facile co-precipitation method and calcined at 700°C. The phase identification carried out by XRD measurements and Raman spectroscopy analysis of calcined powders reveals the formation of mainly anatase phase for undoped TiO₂, and 0.5 mol.% Co-doped TiO₂ whereas rutile phase for 1 mol.% Co-doped TiO₂. The sensors prepared with these powders deposited on interdigital (IDE) sensor platforms were tested toward NO₂ and H₂ sensing properties at 600°C. As the undoped and 0.5% Co-doped TiO₂ reveal n-type behavior, 1% Co-doped TiO₂ shows p-type semi-conductive behavior. One percentage Co-doped TiO₂ exhibits good sensing performance toward NO₂ while the undoped TiO₂ powder yields the best sensor performance toward H₂ at 600°C. This indicates that the crystal structure of TiO₂ sensing material must be adjusted depending on the nature of target gas. The results indicate that the main factor influencing high temperature gas sensor performance of nanoparticulate TiO₂ is either the alteration of its electronic structure or the type of polymorphs.

Keywords: co-precipitation, high-temperature sensor, nitrogen oxides, hydrogen, electronic structure, co-doped TiO₂

OPEN ACCESS

Edited by:

Zoltán Kónya,
University of Szeged, Hungary

Reviewed by:

Josep Albero,
Instituto de Tecnología Química
(ITQ), Spain
Anita Lloyd Spetz,
Linköping University, Sweden

*Correspondence:

Bilge Saruhan
bilge.saruhan@dlr.de

Specialty section:

This article was submitted to
Translational Materials Science,
a section of the journal
Frontiers in Materials

Received: 07 June 2019

Accepted: 25 September 2019

Published: 10 October 2019

Citation:

Lontio Fomekong R and Saruhan B
(2019) Synthesis of Co³⁺ Doped
TiO₂ by Co-precipitation Route and Its
Gas Sensing Properties.
Front. Mater. 6:252.
doi: 10.3389/fmats.2019.00252

HIGHLIGHTS

- Undoped and Co-doped TiO₂ were synthesized by co-precipitation route.
- Cobalt doping of TiO₂ promotes the anatase-rutile transformation.
- Undoped TiO₂ at 600°C, being n-type semiconductor shows the highest response to H₂.
- 1% Co-doped TiO₂ with p-type behavior was more sensitive toward NO₂ at 600°C.

INTRODUCTION

NO_x gas sensors are gaining importance in automotive exhausts and combustion systems. Better performance resistive gas sensors can endure the harsh conditions and act effectively despite the strengthened international legislations. The corresponding gas sensors require durability at high working temperatures (exceeding >> 500°C). Semiconducting metal oxides are ideally used as gas sensing materials in resistive sensors due to their numerous benefits such as reasonably high sensitivity, easy fabrication processes and low cost (Dey, 2018). Most of transition metal oxides, such as SnO₂, WO₃, ZnO, NiO, or CuO used for this purpose display the optimum sensitivity at temperatures below 400°C (Wang et al., 2010). On the other hand, as one of the known

semiconducting oxides, TiO₂ is capable of operating as a gas sensing material at temperatures as high as 600°C (Esmailzadeh et al., 2012). The additional benefits of TiO₂ are non-toxicity, easy fabrication, and the good chemical stability (Chen and Mao, 2007). TiO₂ is a high resistive n-type semiconductor with rather poor conductivity to be adopted for sensing oxidative gases such as NO₂ (Huusko et al., 1993). Previous studies report that this disadvantage can be overcome by conversion of an n-type oxide to p-type semiconductor through addition of low valence dopant atoms to alter the electronic structure. Some previous studies in our team show how the Al and Cr-addition alters the electron conductivity of TiO₂ from n- to p-type leading to effective gas sensing materials. As far as Cr-doped TiO₂ is concerned, the optimum temperature for sensing properties has been limited with 500°C while the Al-doped TiO₂ detects NO₂ at 600°C but the sensitivity is low and the signal converts to p-type at 800°C (Saruhan et al., 2013; Gönüllü et al., 2015). Several other papers discuss the relation and reasons between the nature of the electronic structure and the sensing characteristics of the oxide materials (Wisitsoraat et al., 2009; Zhaohui et al., 2013; Gönüllü et al., 2015) and report that the enhancement of the sensing performance can directly be controlled by adjustment of the electronic structure to p-type at the semi-conducting oxide sensing layer.

In order to understand further if such an alteration can be achieved by Co-doping of TiO₂ and how this may affect the gas sensing behavior of TiO₂, we have synthesized Co-doped TiO₂ nanoparticles by oxalate induced co-precipitation method and produced sensors by depositing the powders on interdigital electrodes. The resulting powders are characterized and the sensors are analyzed to identify their H₂ and NO₂ sensing capabilities. This paper reports, to the best of our knowledge for the first time, the effect of Co³⁺ doping on the high temperature gas sensing behavior of TiO₂.

EXPERIMENTAL

Undoped and Co-doped TiO₂ nanoparticles were synthesized by employing the same processing route. Firstly, the starting precursor solutions were prepared. Cobalt acetate was dissolved in acetic acid as titanium iso-propoxide was diluted separately in absolute ethanol. The cobalt acetate and titanium iso-propoxide solutions were adjusted to obtain 0.5 and 1 mol.% of cobalt in TiO₂ and were labeled as 0.5 Co-doped TiO₂ and 1 Co-doped TiO₂, respectively. These solutions were then mixed to each other and stirred for 5 min. Oxalic acid is utilized for the co-precipitation of a powder from this mixed solution. For that, oxalic acid was dissolved in absolute ethanol solution and poured progressively in to the mixed solution. The resulting mixture was stirred for 1 h to allow the complete precipitation. The so-obtained precipitate was filtered and dried in oven at 80°C yielding a white powder for the undoped and pink colored powder for the Co-doped samples. The as-prepared precursor powder was then calcined for 3 h at 700°C in a muffle furnace under static air.

The XRD diffractograms of the co-precipitated and calcined samples were collected with a D5000 Siemens Kristalloflex O-20 powder diffractometer having Bragg-Brentano geometry. The reflections from the JCPDS database were assigned to the experimental diffractograms by means of the program EVA from BRUKER AXS.

The Raman spectroscopy measurement were carried out at the Applied University of Bonn-Rhein-Sieg on Senterra Raman spectrometer from Bruker under 532 nm and 20 mW by focusing power laser excitation on samples through a 20 x objective. The morphology of the particles was determined by Scanning Electron Microscopy (SEM) analysis using a Zeiss Ultra 55 SEM.

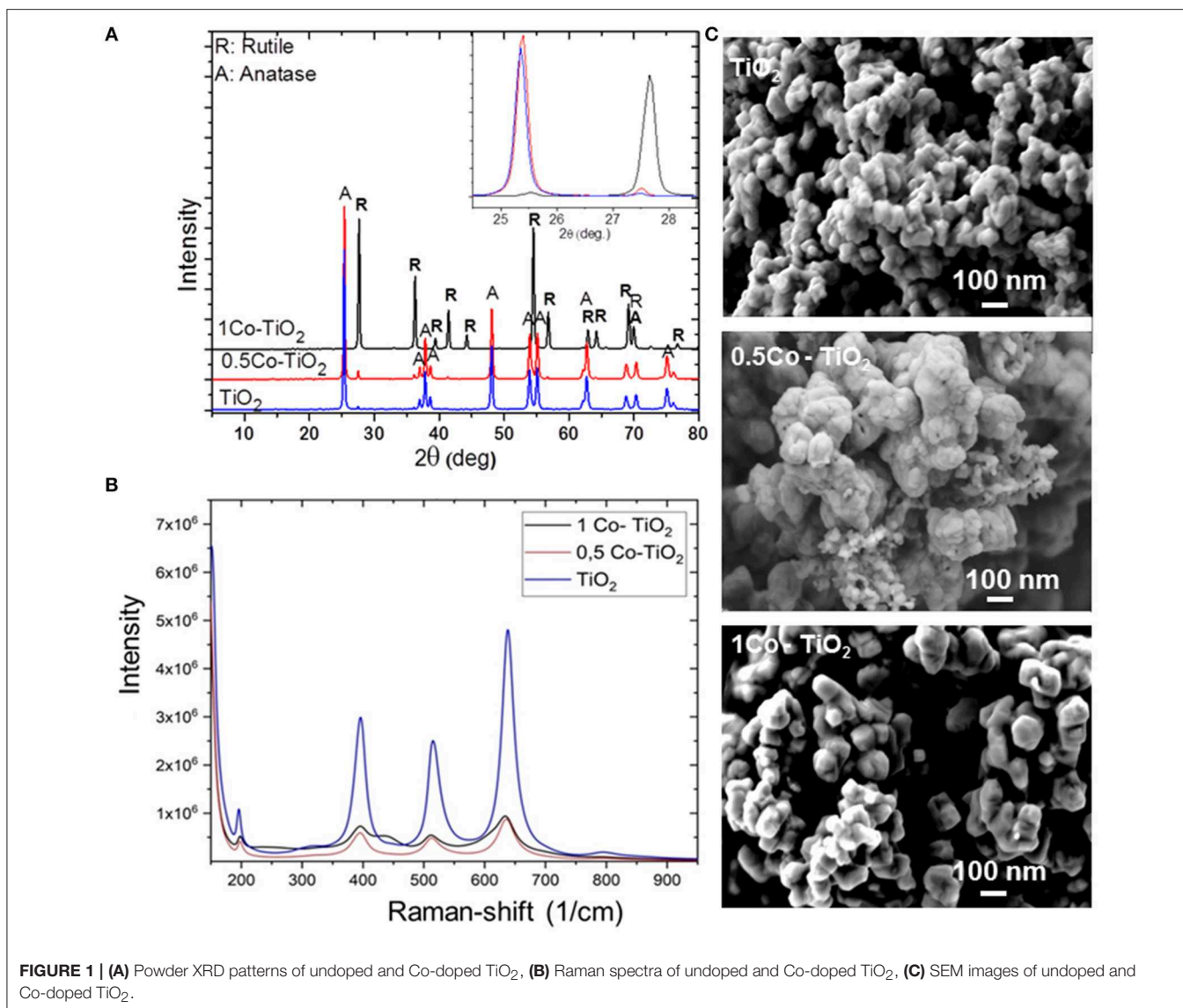
Specific surface area of the samples was determined using Micrometrics Tristar 3,000 equipment using N₂ adsorption at 77.150 K. Samples were degassed under vacuum at 120°C for 2 h prior to the surface area measurements. The specific surface area was calculated using the Brunauer-Emmet-Teller (BET) equation.

The as prepared TiO₂ and Co-doped TiO₂ powders were deposited as thick films using a simple drop-coating method on alumina substrates that were previously fitted with interdigitated electrodes. The sensor measurements were carried out in a specially constructed apparatus consisting of a tube furnace and a custom-built quartz glass reactor providing a thermocouple directed at the specimen. The electrical measurements were performed by using a Keithley 2635A Sourcemeter. The sensor response for n-type semiconductors is defined by $(R_{\text{gas}}/R_{\text{air}} - 1) \times 100$ and $(R_{\text{air}}/R_{\text{gas}} - 1) \times 100$ for oxidizing and reducing gases, respectively, while for p-type semiconductor, $(R_{\text{gas}}/R_{\text{air}} - 1) \times 100$ and $(R_{\text{air}}/R_{\text{gas}} - 1) \times 100$ for reducing and oxidizing gases, respectively.

RESULTS AND DISCUSSIONS

The phase compositions of all synthesized powders were initially investigated by XRD as presented in **Figure 1A**. The undoped and the 0.5 Co-doped TiO₂ samples showed pure TiO₂ consisted of its two polymorphs; anatase (majority, JCPDS 21-1272) and rutile phases (minority, JCPDS 21-127). No other phase containing Co was observed. The amount of rutile phase was found to be slightly higher in 0.5 Co-doped TiO₂ than the undoped one. Also, the 1 Co-doped TiO₂ sample showed only single phase TiO₂ but this time the rutile polymorph was the major phase as anatase phase was in trace amount.

The X-ray results indicated that the cobalt dopant promotes the anatase-to-rutile phase conversion of TiO₂. As presented on the inset of **Figure 1A**, a shift of the 2 Theta angles toward the higher values was observed indicating that the lattice parameters of TiO₂ decreases on Co-addition since according to the Bragg's law equation ($2d\sin\theta = n\lambda$), the lattice parameter is inversely proportional to 2θ . Increasing 2θ angle does indeed mean that the lattice parameter decreases. In fact, the ionic radius of Co³⁺ is smaller than that of Ti⁴⁺ (Co³⁺ = 0.685 Å, Ti⁴⁺ = 0.745 Å). Hence, this leads to the contraction of the TiO₂ unit cell on substitution of Ti⁴⁺ through Co³⁺. If otherwise, the substitution occurs through the incorporation of Co²⁺, an



opposite change in the lattice parameter would be expected (i.e., 2 Theta angles shift to lower values). Since Co²⁺ has a larger ionic radius (Co²⁺ = 0.79 Å) than that of Ti⁴⁺, an expansion of the TiO₂ unit cell shall occur yielding an increase of the lattice parameters. Chanda et al. has proven this assumption through their structural and magnetic studies on Co-doped TiO₂ (Chanda et al., 2018). Thus, it is plausible to consider in the present case that the substitution of Ti⁴⁺ sites occurs by smaller ionic radius Co³⁺ leading to a volume reduction of TiO₂-lattice. Therefore, an overall volume contraction of ~8% is reasonable to obtain through Co³⁺-doping of TiO₂. This promotes the conversion of anatase to rutile because the reconstructive anatase-to-rutile transformation involves a contraction of the c-axis (Hanaor and Sorrell, 2011).

Figure 1B displays the Raman spectra of the samples that were obtained between the wavenumbers of 200–900 cm⁻¹. The Raman lines at 197, 390, 511, 637 cm⁻¹ can be assigned to E_g, B_{1g},

A_{1g}, or B_{1g}, and E_g modes of anatase phase, respectively, which confirm that the phase condition of our Co-doped TiO₂ samples belongs to the tetragonal form of anatase phase. Moreover, the spectra show that the peak intensities decrease drastically after doping. As XRD results showed that the main phase for 0.5 Co-doped TiO₂ is anatase, the decrease of intensity observed in the Raman spectra can be attributed to the increase of oxygen vacancies which occurred through the substitution of Ti⁴⁺ by Co³⁺ to balance the charge neutrality, relying on the difference between their ionic charges. These vacancies lead to the lattice distortion and results in a change of the diffraction intensity. Similar results were reported by Chanda et al. (2018). On the other hand, the XRD measurement revealed that the sample 1 Co-doped TiO₂ contains rutile as the major polymorph as anatase was only present in a very small quantity. This may explain the decrease observed at the Raman spectra of this composition. Moreover, the Raman spectra of 1 Co-doped TiO₂

yielded a smaller shift toward lower wavelengths while new peaks (436 cm^{-1}) appeared indicating the presence of rutile polymorph, as mentioned in literature (Niilisk et al., 2006).

Figure 1C shows the morphology of the synthesized powders. The microscopic investigation revealed the formation of spherical nanoparticles with sizes around 70 nm that tend to agglomerate at the undoped powder samples. Doping with Co appears to influence the powder morphology. As the sample 0.5 Co-doped TiO₂ shows more agglomerated spherical particles, the sample 1 Co-doped TiO₂ presented larger and well-faceted rhombohedral crystallites with less agglomeration.

The BET-measured specific surface area of the synthesized samples were 8, 7, and 4 m²/g for undoped TiO₂, 0.5 Co-doped TiO₂, and 1 Co-doped TiO₂, respectively. The surface area decreases with the increasing cobalt content, as the greatest decrease being with the 1 Co-doped TiO₂ that corresponds to the particle size increase as observed by SEM analysis (see **Figure 1C**).

The sensing properties of the undoped and doped TiO₂ were investigated toward 200 ppm NO₂ and 200 ppm H₂ at 600°C using synthetic air as carrier gas. This temperature

was chosen on the basis of our previous results obtained with undoped and Al- and Cr-doped TiO₂ relying on the fact that undoped TiO₂ is capable of NO₂-sensing at above 400°C (Saruhan et al., 2013; Gönüllü et al., 2015). In fact, as the temperature increases, the sensor signal and also the response time decreases. Accordingly, our present results indicate that the equilibrium temperature for sensing is at 600°C. Additionally, it is known that the TiO₂ polymorphs will change at temperatures above 700°C. In order to avoid any temperature-induced complexity related to polymorph and electronic structures and to emphasize the effect of Co-dopant on the sensing properties, the operating temperature has been kept below 700°C.

As **Figure 2A** shows, the sensors yield higher response toward H₂ than NO₂. The H₂ sensor responses are 42, 23, and 33% for undoped, 0.5 Co-doped TiO₂ and 1 Co-doped TiO₂, respectively. The undoped sample shows the highest response toward H₂. The presence of Co-dopant seems to decrease the H₂-sensing performance of TiO₂ even though doping creates more oxygen vacancies in TiO₂. This behavior can be attributed to the increase of rutile polymorph content on doping with cobalt, as previously reported, rutile is the less active (in term of functional properties)

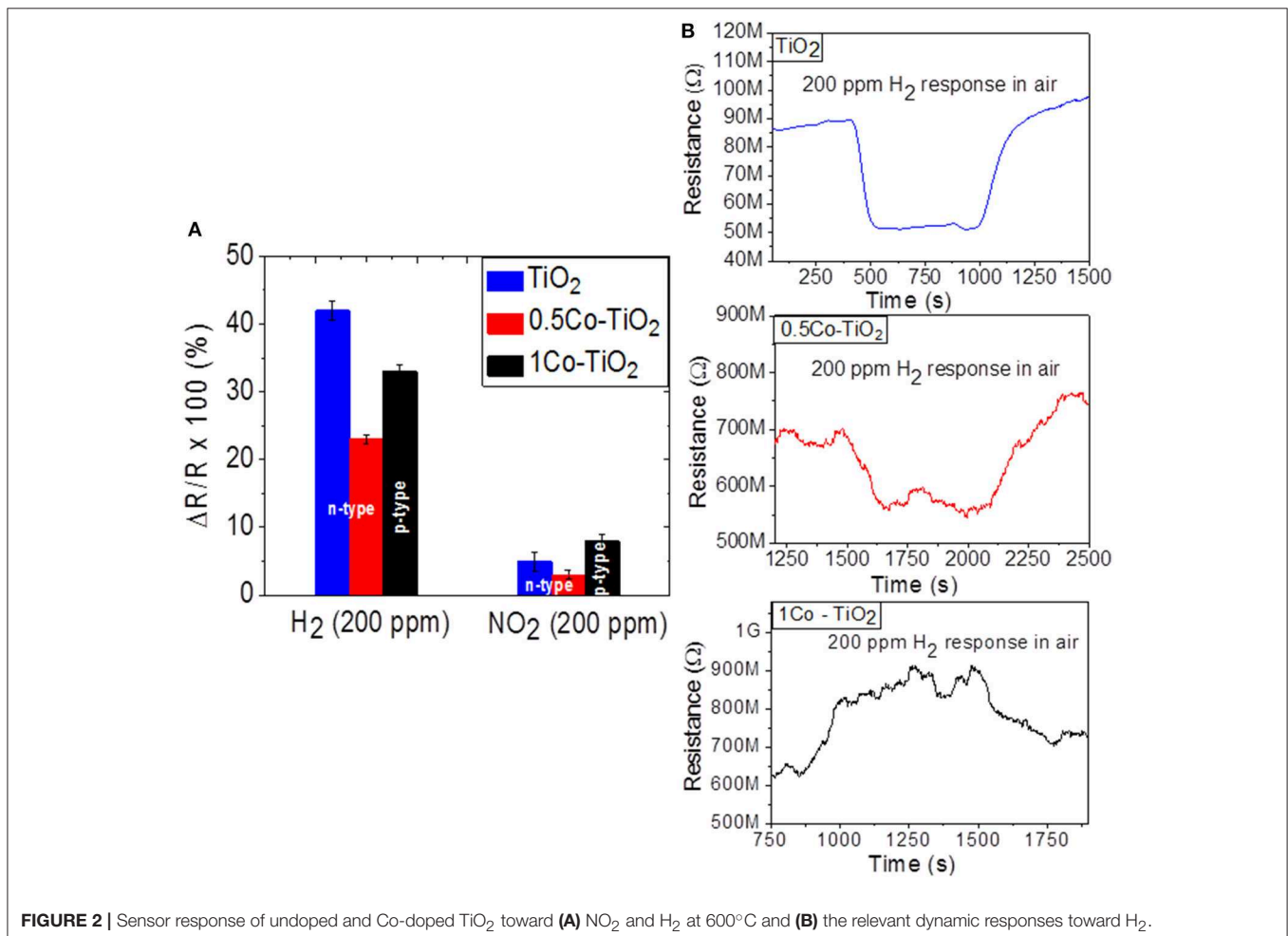


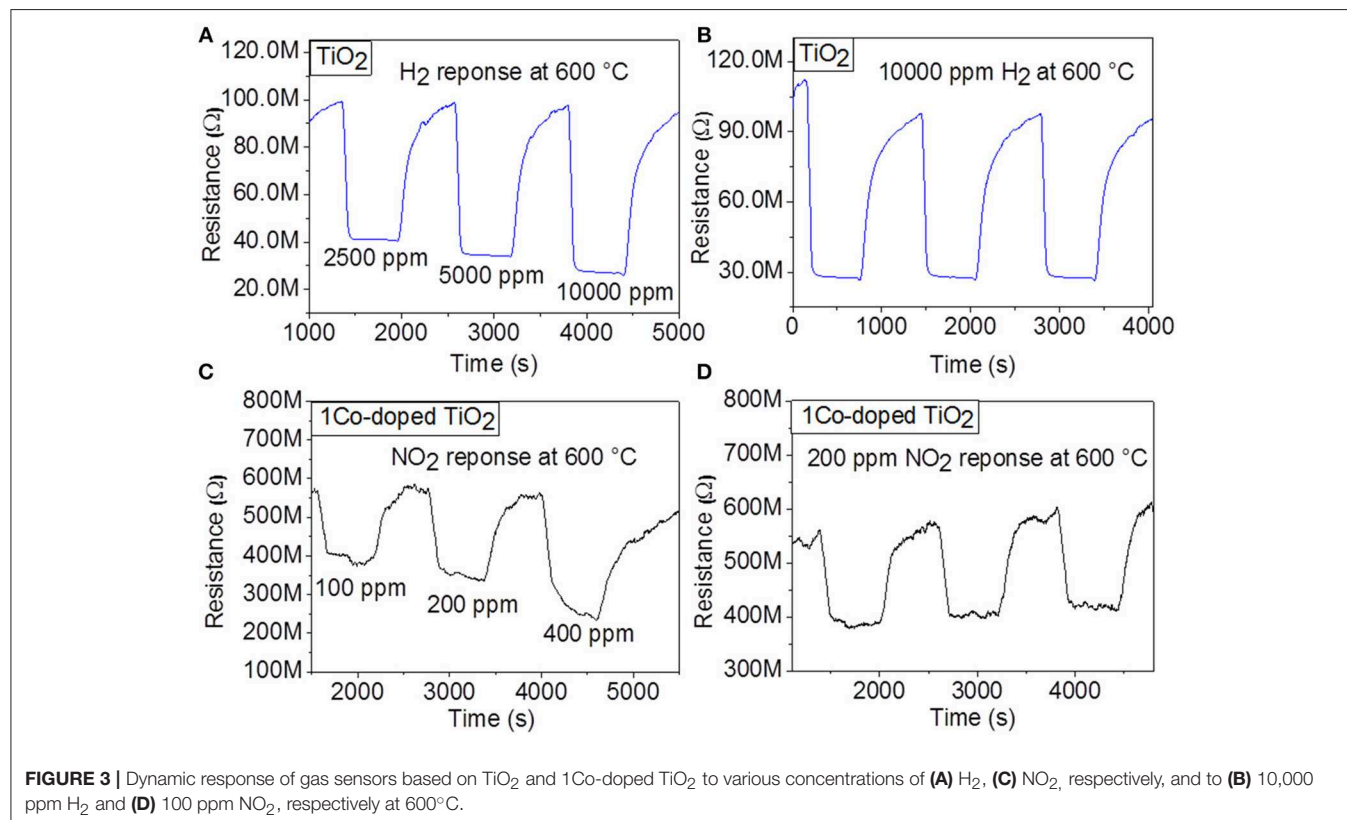
FIGURE 2 | Sensor response of undoped and Co-doped TiO₂ toward **(A)** NO₂ and H₂ at 600°C and **(B)** the relevant dynamic responses toward H₂.

polymorph of TiO₂ (Luttrell et al., 2014). On the other hand, the 1 Co-doped TiO₂ which contains predominantly rutile polymorph showed a higher response toward H₂ than 0.5 Co-doped TiO₂. This discrepancy can be explained by alteration of the conductivity from n-type to p-type. In fact the dynamic response of the sensors toward H₂ given in **Figure 2B** reveals that undoped and 0.5 Co-doped TiO₂ exhibit n-type semi-conductivity (i.e., their electrical resistance decreases upon interaction with hydrogen) while the 1 Co-doped TiO₂ yields p-type conductivity (its electrical resistance increases when reducing gas is introduced).

The sensor responses measured toward the oxidizing gas NO₂ were 5, 3, and 8% for undoped, 0.5 Co-doped TiO₂ and 1 Co-doped TiO₂, respectively. In the case of NO₂ sensing, the 1 Co-doped TiO₂ showed the highest response. This may be mainly due to the electronic alteration of TiO₂ from n to p-type semiconductor. Previous literature points out that this alteration can be utilized for the detection of oxidizing gas (Huusko et al., 1993). Our current results confirm that the dominant factor for the gas sensing property of the Co-doped TiO₂ depend on the existing polymorphs as well as the nature of target gas (oxidizing or reducing). In the case of reducing gases, the type of polymorphs has more influence on the gas sensitivity than the type of electronic structure, while an opposite trend can be observed for oxidizing gases.

Considering these preliminary results, sensing properties of the undoped TiO₂ toward H₂ and of 1 Co-doped TiO₂ toward

NO₂ are further investigated at 600°C. **Figures 3A,C** display the dynamic response of the sensor with undoped TiO₂ at 600°C to various H₂ concentrations (2,500, 5,000, and 10,000 ppm) and those with 1 Co-doped TiO₂ to various NO₂ concentrations (100, 200, and 400 ppm), respectively. As these response measurements exhibit, upon gas exposure, the sensor reaches to an equilibrium resistance value and settles back almost to the original baseline resistance value when the test gas is vented. This sequence has been reproduced for all the applied gas concentrations, demonstrating very good reproducibility and stability at the sensor behavior. For undoped TiO₂, the calculated sensor signals were 58% for 2,500, 64% for 5,000, and 72% for 10,000 ppm of H₂, while for 1 Co-doped TiO₂, the sensing signal was 32% for 100, 40% for 200, and 55% for 400 ppm of NO₂, respectively. These investigations indicate that the gas response increases with increasing concentration of NO₂ suggesting the capability of the sensor for quantitative analysis. In order to confirm the stability and reproducibility of the synthesized undoped TiO₂ and 1 Co-doped TiO₂ powders at the same H₂ and NO₂ concentrations, respectively, the sensor tests were repeated by introducing into the test chamber three times 10,000 ppm H₂ (for undoped TiO₂) and 200 ppm NO₂ (for 1 Co-doped TiO₂) under the same test conditions. The dynamic curves of these investigations are shown in **Figures 3B,D**. The average value of the gas response is 70% for H₂ and 38% for NO₂ for undoped TiO₂ and 1 Co-doped TiO₂ respectively, with a negligible deviation. Even though the baseline resistance changes slightly with time, the stability of the sensors is maintained well.



CONCLUSION

This paper reports the successful synthesis of undoped and Co-doped TiO₂ nanoparticles by a facile co-precipitation route through the use of oxalic acid. According to the X-ray diffraction and Raman spectroscopy analysis, the substitution of Ti⁴⁺ by Co³⁺ creates oxygen vacancies and promotes the anatase-to-rutile transformation. The sample 1 Co-doped TiO₂ which reveals p-type conductive behavior yields an enhanced NO₂ response at 600°C under air as carrier gas. However, the undoped TiO₂ shows n-type semiconductor behavior with the highest sensor response toward H₂ at 600°C. The enhancement of high temperature NO₂ sensing performance is related to the alteration in electronic structure as well as the formation of rutile polymorph in the 1 Co-doped TiO₂ sample. It has been a remarkable effect to obtain two different behaviors by only addition of very small quantities of Co-dopant to TiO₂ under the same processing conditions. If the Co-dopant content exceeds 1%, CoTiO₃ starts to form as a secondary phase introducing a new parameter to take into consideration. For the perspective of NO₂ sensing

optimization, Co-dopant contents between 0.5 and 1 mol.% may also be considered.

DATA AVAILABILITY STATEMENT

All datasets generated for this study are included in the manuscript/supplementary files.

AUTHOR CONTRIBUTIONS

RL has synthesized and characterized the material for sensor application. BS have initiated the idea of applying the Co-dopant to TiO₂ and gave feedback in evaluating the sensing mechanism with this material.

ACKNOWLEDGMENTS

The authors thank Rene Breuch and Johannes Warmer of H-BRS for Raman Spectroscopy measurements. The grant provided by the DLR-DAAD Fellowship program under no. 284 is acknowledged.

REFERENCES

- Chanda, A., Rout, K., Vasundhara, M., Joshi, S. R., and Singh, J. (2018). Structural and magnetic study of undoped and cobalt doped TiO₂ nanoparticles. *RSC Adv.* 8, 10939–10947. doi: 10.1039/C8RA00626A
- Chen, X., and Mao, S. (2007). Titanium dioxide nanomaterials: synthesis, properties, modifications, and applications. *Chem. Rev.* 107, 2891–2959. doi: 10.1021/cr0500535
- Dey, A. (2018). Semiconductor metal oxide gas sensors: a review. *Mater. Sci. Eng. B* 229, 206–217. doi: 10.1016/j.mseb.2017.12.036
- Esmailzadeh, J., Marzbanrad, E., Zamani, C., and Raissi, B. (2012). Fabrication of undoped-TiO₂ nanostructure-based NO₂ high temperature gas sensor using low frequency AC electrophoretic deposition method. *Sens. Actuat. B* 161, 401–405. doi: 10.1016/j.snb.2011.10.051
- Gönüllü, Y., Haidry, A. A., and Saruhan, B. (2015). Nanotubular Cr-doped TiO₂ for use as high-temperature NO₂ gas sensor. *Sens. Actuat. B* 217, 78–87. doi: 10.1016/j.snb.2014.11.065
- Hanaor, D. A. H., and Sorrell, C. C. (2011). Review of the anatase to rutile phase transformation. *J. Mater. Sci.* 46, 855–874. doi: 10.1007/s10853-010-5113-0
- Huusko, J., Lantto, V., and Torvela, H. (1993). TiO₂, thick-film gas sensors and their suitability for NO_x monitoring. *Sens. Actuat. B* 16, 245–248. doi: 10.1016/0925-4005(93)85188-G
- Luttrell, T., Halpegamage, S., Tao, J., Kramer, A., Sutter, E., and Batzill, M. (2014). Why is anatase a better photocatalyst than rutile? Model studies on epitaxial TiO₂ films. *Sci. Rep.* 4:4043. doi: 10.1038/srep04043
- Nilisk, A., Moppel, M., Pärs, M., Sildos, I., Jantson, T., Avarmaa, T., et al. (2006). Structural study of TiO₂ thin films by micro-Raman spectroscopy. *Cent. Eur. J. Phys.* 4, 105–116. doi: 10.1007/s11534-005-0009-3
- Saruhan, B., Yüce, A., Gönüllü, Y., and Kelm, K. (2013). Effect of Al doping on NO₂ gas sensing of TiO₂ at elevated temperatures. *Sens. Actuat. B* 187, 586–597. doi: 10.1016/j.snb.2013.04.111
- Wang, C., Yin, L., Zhang, L., Xiang, D., and Gao, R. (2010). Metal oxide gas sensors: sensitivity and influencing factors. *Sensors* 10, 2088–2106. doi: 10.3390/s100302088
- Wisitsoraat, A., Tuantranont, A., Comini, E., Sberveglieri, G., and Wlodarski, W. (2009). Characterization of n-type and p-type semiconductor gas sensors based on NiO_x doped TiO₂ thin films. *Thin Solid Films* 517, 2775–2780. doi: 10.1016/j.tsf.2008.10.090
- Zhaohui, L., Dongyan, D., and Congqin, N. Li Z., Ding D., Ning C. (2013). p-type hydrogen sensing with Al- and V-doped TiO₂ nanostructures. *Nanoscale Res. Lett.* 8:25. doi: 10.1186/1556-276X-8-25

Conflict of Interest: The authors declare that the research was conducted in the absence of any commercial or financial relationships that could be construed as a potential conflict of interest.

Copyright © 2019 Lontio Fomekong and Saruhan. This is an open-access article distributed under the terms of the Creative Commons Attribution License (CC BY). The use, distribution or reproduction in other forums is permitted, provided the original author(s) and the copyright owner(s) are credited and that the original publication in this journal is cited, in accordance with accepted academic practice. No use, distribution or reproduction is permitted which does not comply with these terms.